Nonlinear optics in ultra high Q microcavity

Term paper for Phy 566 Nonliear Optics by Shoufeng Lan

1. Introduction

Optical microcavities are used to confine light both spatially and temporally. The long photon lifetimes and small mode volume of ultra-high-Q microcavities, allow to significantly reduce the threshold for nonlinear phenomena. Early work recognized these attributes through many stimulated nonlinear phenomena, such as stimulated Brillouin scattering[1], stimulated Raman scattering[2] and cascaded Raman scattering[3] in liquids formed from Raman active media such as CS_2. However, due to the inefficient nature of free space laser excitation used in these experiments, as well as due to the transient nature of the microdroplets, they required high threshold pump powers and did not allow stable and long term study of nonlinear optical effects.

In this paper, we report a micrometer-scale nonlinear Raman source using a taper-fiber coupled silica microsphere. The Raman scattering has a highly efficient pump-signal conversion (higher than 35%) in this case and pump thresholds nearly 1000 times lower than shown before. This reduction of necessary pump power is due to the efficient and optimum coupling to ultra-high-Q optical modes. This allows the authors to observe stimulated Raman scattering at threshold levels as low as 65μW, which is usually considered the regime of linear optics. Due to the high conversion efficiency the internal Raman fields can reach power levels which are sufficient to generate higher order Raman fields. In addition, geometrical control of recently develop toroid micocavities enables a transition from stimulated to optical parametric oscillation regimes. So we report a fiber coupled toroidal microcavity as a parametric oscillator [4] as well.

2. Theoretical analysis

2.1 Optical modes in fiber coupled microcavities

The optical modes of a spherical dielectric particle can be calculated by solving Helmholtz equation in spherical coordinates. The field distribution and the resonance locations are determined by matching the solutions interior and exterior to the sphere at the dielectric-air boundary[5], leading to a characteristic equation. For a microsphere this requires matching the Bessel function $j_l(ka)$ and the outgoing Hankel functions $h_l(ka)$ at the dielectric boundary. The characteristic equation for this case is given by:

$$x \cdot \frac{j_l'(ka)}{j_l(ka)} = \frac{h_l'(ka)}{h_l(ka)} \quad \text{where } x = \begin{bmatrix} \frac{1}{m} \text{ for TM} \\ m \text{ for TE} \end{bmatrix}$$

On the other hand, the optical modes of a tapered optical fiber can be approximated

by the modes of a dielectric cylinder. Particularly important in the context of taper fiber coupling is the fraction of energy which is outside the tapered fiber. With slowly varying envelope approximation, the coupling from a resonator to a waveguide is fundamentally described by three parameters, the resonant frequency ω_0, the decay rate $1/\tau_0$ of the mode due to internal cavity losses, and the cavity decay rate $1/\tau_{ex}$ due to coupling to the waveguide mode.

2.2 Raman scattering in fiber taper coupled microcavities

In the conventional treatments, the pump and Raman waves are assumed to be plane waves, with only one spatially varying variable, simplifying considerably the coupled wave-equations. In the case of a microcavity, the fields involved are the whispering-gallery modes. By reformulating the wave-equation one arrives at a similar set of equations as in the case of plane waves, however with modified coupling coefficients, which take into account the coupling among different WG-modes. This treatment leads to the definition of overlap factors (or alternatively stated to the definition of the effective mode area, or effective mode volume). The plane wave interaction in the terms of the electric field is described by:

$$\frac{d}{dz}\vec{E}_p = -\frac{1}{2}\left(\frac{\omega_p}{\omega_R}\right)\left(\frac{c}{n_{eff}}\right) g_R \left|\vec{E}_R\right|^2 \vec{E}_p$$

$$\frac{d}{dz}\vec{E}_R = \frac{1}{2} g_R \left(\frac{c}{n_{eff}}\right) \left|\vec{E}_p\right|^2 \vec{E}_R$$

In these equations the bulk Raman gain coefficient is given by g_R and is well known for silica fibers. Reform the eqatuions with a WGM in the waveguide coupled microcavity, we can simplify the equation as follow. We assume that the pump wavelength and the Raman wave are on resonance and use the slowly varying envelope approximation.

$$\frac{dA_p}{dt} = -\left(\frac{1}{2\tau_{ex}} + \frac{1}{2\tau_0}\right)_p A_p - \frac{\omega_p}{\omega_R} g_R^c \cdot |A_R|^2 A_p + \sqrt{\frac{1}{\tau_{ex}}} s$$

$$\frac{dA_R}{dt} = -\left(\frac{1}{2\tau_{ex}} + \frac{1}{2\tau_0}\right)_R A_R + g_R^c \cdot |A_P|^2 A_R$$

Here ‘A’ signifies the slowly-varying amplitude of the pump and Raman WGM of the cavity and denotes the input wave. The excitation frequency of the pump mode and resonant Raman mode is given by ω_R and ωp and τ is the total lifetime of photons in the resonator, which is related to the quality factor by $Q = \omega \cdot \tau$ The coupling coefficient $\kappa = (1/\tau_{ex})^{1/2}$ denotes the coupling of the input pump wave s to the cavity whispering-gallery-mode [6]. The Raman intra-cavity gain coefficient is denoted as g_R^C, which is related to the more commonly used gain coefficient g_R (measured in units of m/*Watt*) by integration over the mode area.

The first Raman field can itself act as a secondary pump field and generate further Raman modes. This process of cascaded Raman scattering can be described by

including higher order coupling terms into the coupled mode equations of pump and Raman fields as shown below

$$\frac{dE_{RN}}{dt} = \left[-\left(\frac{1}{2\tau_t}\right)_{RN} + g^c_{RN} \left| E_{R(N-1)} \right|^2 \right] E_{RN}$$

The general solutions for the threshold of the even and odd order Nth Raman modes are given by the following expressions.

$$P_t^{N=2m+1} = \frac{1}{C(\Gamma)} \frac{\pi^2 n^2}{g_R \lambda_p \lambda_R} V_{eff} \frac{1}{Q_0^2} \frac{(1+K)^3}{K} \cdot \frac{(N+1)^3}{8}$$

$$P_t^{N=2m} = \frac{1}{C(\Gamma)} \frac{\pi^2 n^2}{g_R \lambda_p \lambda_R} V_{eff} \frac{1}{Q_0^2} \frac{(1+K)^3}{K} \cdot \frac{N^2(N+2)^2}{8}$$

2.3 Optical parametric oscillator in fiber taper coupled microcavities

Optical parametric oscillators (OPOs) rely on energy and momentum conserving optical processes to generate light at new "signal" and "idler" frequencies. In WG type resonators, such as microtoroids, momentum is intrinsically conserved when signal and idler angular mode numbers are symmetrically located with respect to the pump mode (i.e. l_S, l_I=l_P±N)

$$2\beta_m = \beta_{m+N} + \beta_{m-N}$$

$$2\frac{m}{R_0} = \frac{m-N}{R_0} + \frac{m+N}{R_0}$$

Energy conservation ($2\hbar\omega_P = \hbar\omega_S + \hbar\omega_I$), on the other hand, is not expected to be satisfied a priori, since the resonant frequencies are, in general, irregularly spaced due to both cavity and material dispersion. As a result, the parametric gain is a function of the frequency detuning,

$$\Delta\omega = 2\omega_p - \omega_S - \omega_I$$

which effectively gives the degree to which the interaction violates strict energy conservation. In the case of silica, the material dispersion of silica in the 1500 nm band leads to a positive detuning frequency. It can be shown that the existence of parametric gain requires that this detuning be less than the parametric gain bandwidth[7] $\Omega = 4 \sqrt{c/n}\, \gamma P$ ($\gamma = \omega/c \, \frac{n_2}{A_{eff}}$)where $n_2 \approx 2.2 \times 10^{-20}$ m^2/W is the Kerr nonlinearity for silica [8] and P is the circulating power within the micro-cavity. The effective nonlinearity γ depends on inversely on the effective cross section of the mode. By equating parametric gain and micro-cavity loss (as determined by loaded Q factor), the threshold pump power necessary in the waveguide is obtained for parametric oscillation.

$$P_t^{Kerr} = \frac{\omega_0^2 Q_0^{-2} (1+K)^2 + (\Delta\omega/2)^2}{2\gamma\Delta\omega\,(c/n_{eff})} \cdot \frac{\pi^2 R n_{eff}}{C(\Gamma)\lambda_0} \frac{(K+1)^2}{Q_0 K}$$

To bring about the condition $0 < \Delta\omega < \Omega$ a reduction of the toroidal crosssectional

area reduces the modal effective area Aef f and produces a two-fold benefit. First, it increases the parametric bandwidth Ω through its dependence on γ [7] and second, it reduces Δω.

4. Result spectrums for Raman scattering in microcavities

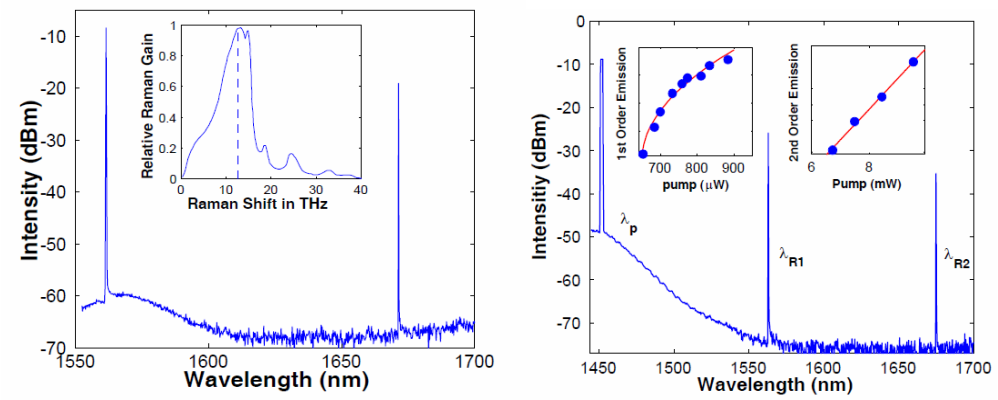

(1) (2)

Figure 2.1: (1)Single longitudinal mode Raman lasing. Raman spectrum for a 40 mm diameter microsphere. (2) Cascaded Raman scattering in a 58μm diameter microcavity. The insets show the pump-to-Raman conversion for first (left inset) and second order (right inset) Raman modes (measured on different microcavities). Solid lines: A theoretical fit.

Stimulated Raman oscillation was observed by pumping a single WGM and monitoring the transmission using an optical spectrum analyzer. Once the threshold for SRS was exceeded, lasing modes in the 1650 nm band could be observed, in correspondence with the peak Raman gain which occurs down-shifted in frequency by approximately 14 THz relative to the pump frequency (wavelength shift of approximately 110 nm). The presence of Raman scattering in microspheres leads to the possibility of generating higher order Raman modes by cascade. By using a shorter pump laser (located at around 1450 nm) cascaded Raman scattering was indeed observed. Figure 2.1(2) shows a typical cascaded Raman spectrum, with a second order Raman mode appearing in the 1650 nm band, two phonon frequencies shifted from the pump. The pump-to-Raman conversion characteristics for first order Raman scattering and the 2nd order Raman mode are shown in the inset. It can be seen that the first order mode does indeed exhibit a square-root dependence on the launched pump power. The 2nd order Raman mode, in contrast, exhibits the expected linear increase with pump power.

As stimulated Raman scattering does not depend on the detuning frequency (i.e. it is intrinsically phase-matched), it is the dominant nonlinear mechanism by which light is generated for large detuning values. With decreasing Δω, a transition from stimulated to parametric regimes occurs when the threshold for parametric oscillation falls below that for Raman (The peak parametric gain is larger than the peak Raman gain, $g_{Kerr}^{Max} \approx 2\, g_{R}^{Max}$ [8]). Also note that for increased waveguide loading (and hence

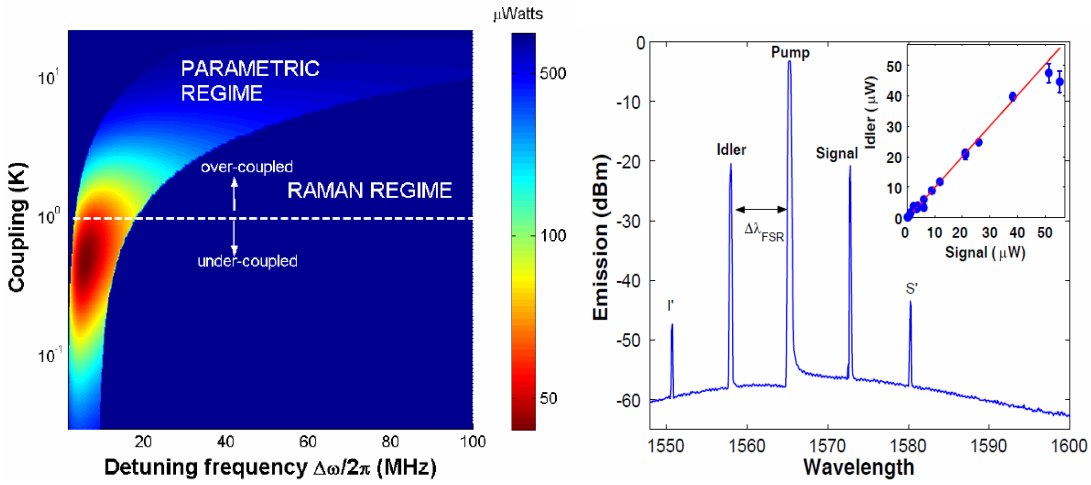

(1) (2)

Figure 10.3: (1)Nonlinear processes in a microcavity with D=50μm, d=4μm and $Q_0=10^8$. (2)Parametric-oscillation spectrum measured for a 67 μm diameter toroidal microcavity.

correspondingly higher threshold pump powers) the transition can be made to occur for detuning values that are progressively larger. For Figure 10.3 (2), the pump is located at 1565 nm and power levels are far above threshold. The signal and idler are modes with successive angular mode numbers and are spaced by twice the free spectral range (2×7.6 nm). The subsidiary peaks (denoted I',S') only appeared at high pump powers and are due to a combination of nonlinear effects, such as parametric oscillation (of signal and idler) as well as four-wave-mixing involving the idler, pump and signal. Inset: idler emission power plotted versus the signal emission power, recorded for different pump powers. The idler-to-signal power ratio is 0.97±0.03. For higher pump powers deviation is observed due to appearance of secondary oscillation peaks (I',S') (compare with main figure).

5. Summary

In summary, first order and cascaded Raman scattering in microspheres are discussed in waveguide-coupled microcavities. A theoretical analysis was presented using the coupled mode equations for the pump and Raman WGMs. Using these equations, the threshold condition for stimulated Raman scattering was derived. This analysis revealed that odd and even order Raman lines exhibit different pump-to-Raman emission characteristics. Even order Stokes fields are found to exhibit a linear increase in generated Raman power as a function of pump power, whereas odd-order Stokes fields exhibit a square root dependence. Optical parametric oscillation in high Q microtoroid is reported as well. By using the geometric of microtoroid, which has much more confined mode area, the phase matching condition for OPO was satisfied. The author claimed that it is observed for the first time Kerr-nonliearity induced OPO in a microcavity.

Reference:

1. J. Z. Zhang and R. K. Chang. Generation and suppression of stimulated brillouin-scattering in single liquid droplets. Journal of the Optical Society of America B-Optical Physics, 6(2):151-153, 1989.
2. S. X. Qian, J. B. Snow, and R. K. Chang. Coherent raman mixing and coherent anti-stokes raman-scattering from individual micrometer-size droplets. Optics Letters, 10(10):499-501, 1985.
3. S. X. Qian and R. K. Chang. Multiorder stokes emission from micrometer-size droplets. Physical Review Letters, 56:926-929, 1986.
4. T.J.Kippenberg, Nonlinear optics in ultra high Q whispering gallery optical microcavities. 2004
5. B. E. Little, J. P. Laine, and H. A. Haus. Analytic theory of coupling from tapered fibers and half-blocks into microsphere resonators. Journal of Lightwave Technology, 17(4):704-715, 1999.
6. H.A. Haus. Waves and Fields in Optoelectronics. Prentice-Hall, Englewood Cliffs, NJ, 1984.
7. R. H. Stolen and J. E. Bjorkholm. Parametric amplification and frequency conversion in optical fibers. Ieee Journal of Quantum Electronics, 18(7):1062-1072, 1982. NW199 IEEE J QUANTUM ELECTRON.
8. Robert W. Boyd. Nonlinear optics. Academic Press, Boston, 1992.